6th Congress of Alps-Adria Acoustics Assosiation
16.-17. October 2014
Graz, Austria

Austrian Acoustics Association
Österreichische Gesellschaft für Akustik

Alps Adria Acoustics Association

ISBN: 978-3-200-03921-6

Identifying Cracks in Gears by Bi-Orthogonal Wavelets

Ales Belsak , Jurij Prezelj

ales.belsak@um.si, jurij.prezelj@uni.lj-fs.si

Abstract: *Many damages and faults can cause problems in gear unit operation. A crack in the tooth root is probably the least desirable among them. It often leads to failure of gear unit operation. The analyses and methods of fault detection presented in this paper are based on signals produced by a faultless gear and by a gear with a crack in the tooth root, caused through real operating conditions. A test plant was used to measure these signals. By monitoring vibrations, it is possible to determine the presence of a crack. The influences of a crack in a single-stage gear unit on produced vibrations are presented. Important changes in tooth stiffness are caused by a fatigue crack in the tooth root, whereas, when it comes to other faults, changes of other dynamic parameters are more expressed. Time Frequency Analysis tools, e.g. Wavelets Analyses, were used to perform the analysis of a non-stationary signal.*

Key words: Gear, Failure, Crack, Vibration, Signal analysis

1. INTRODUCTION

The aim of maintenance is to keep a technical system (gear-unit) in the most suitable working condition, and its purpose is to discover, to diagnose, to foresee, to prevent and to eliminate damages. The purpose of modern maintenance, however, is not only to eliminate failures but also to define the stage of a potential danger of a sudden failure of system operation. The aim of diagnostics is to define the current condition of the system and the location, shape and reason of damage formation. The following diagnostic values are used to define incorrect operation, the possibility and location of damages and the possibility of elimination of these damages: different signals, condition parameters and other indirect signs. Identification of the form of damage is based on deviations from the values typical of a faultless gear system. This paper is a continuation of the research presented in [1]. Its aim is to locate a crack more precisely.

A gear unit consists of elements enabling the transmission of rotating movement. Although a gear unit is a complex dynamic model, its movement is usually periodical; faults and damages represent a disturbing quantity or impulse. Local and time changes in vibration signals indicate the disturbance [2,3] and it is possible to expect time-frequency changes [4]. This idea is based on kinematics and operating characteristics [5,6].

The appearance of individual frequency components in signals is often only occasional. It is impossible to find out when certain frequencies appear in the spectrum on the basis of classical frequency analysis of such signals. It is, however, possible to use time-frequency analysis to establish in what way frequency components of non-stationary signals change with time and to determine their intensity levels.

2. INTRODUCTION

The continuous wavelet transform of function $x(t) \in L2(\Re)$ at the time and scale is expressed as follows [10]:

$$W\ x(u,s) = \int_{-\infty}^{+\infty} x(t) \cdot \frac{1}{\sqrt{s}} \cdot \psi^* \left(\frac{t-u}{s} \right) \cdot dt \quad (1)$$

$$\overline{\psi}_s(t) = \frac{1}{\sqrt{s}} \cdot \psi^* \left(\frac{-t}{s} \right) \quad (2)$$

$$\overline{\Psi}_s(\omega) = \sqrt{s} \cdot \Psi^* (s \cdot \omega) \quad (3)$$

where the transform is presented as the product of convolution; Eq. (2) presents the expression of an average wavelet function and the corresponding Fourier integral transform, Eq. (3).

At the continuous wavelet transform, the observed function x(t) is multiplied by a group of shifted and scaled wavelet functions. A simultaneous change in time and

frequency dissemination of the continuous wavelet transform can be observed. Wavelets, as locally limited functions, are used to analyse the observed function x(t), the continuous wavelet transform is very sensitive to local non-stationarities.
Morlet wavelet function, which is a representative of a non-orthogonal wavelet function:

$$\psi_{Morlet}(t,\sigma,\eta)=\frac{1}{\sqrt[4]{\pi}}\cdot e^{-\frac{t^2}{2}}\cdot e^{i\cdot\eta\cdot t} \quad (4)$$

Eq. (5) yields a family of wavelet functions, or a shifted u and scaled s Morlet wavelet function:

$$\psi_{Morlet}(t,\sigma,\eta)=\frac{1}{\sqrt{s}}\cdot\frac{1}{\sqrt[4]{\pi}}\cdot e^{-\frac{1}{2}\cdot\left(\frac{t-u}{s}\right)}\cdot e^{i\cdot\eta\cdot\left(\frac{t-u}{s}\right)} \quad (5)$$

Various wavelet basis functions were selected in wavelet applications. Theoretically speaking, any function that is finite in time and frequency can be used for the basis function. Several types of functions can be used as a wavelet basis; the selection depends on the application-related requirements [18–19].
The Morlet wavelet was used as the basis function due to the similarity of formulation with Gabor transform function that was investigated in our laboratory. The Gabor transform has some particularity in Fourier transforms. The only difference between the Morlet wavelet and Gabor transform is in the exponent term, which helps determine the shape of the wavelet.
Using the expression in Eq. (5), the time function can be further transformed to the frequency domain as shown below:

$$\hat{\psi}_{Morlet}(\omega,\sigma)=\sqrt[4]{\pi}\cdot\sqrt{\frac{2\cdot\pi}{s}}\cdot e^{-i\cdot\omega\cdot u}\cdot e^{-\left(\omega-\frac{\eta}{s}\right)^2\cdot\frac{s^2}{2}} \quad (6)$$

The Morlet wavelet is a complex wavelet and it can be decomposed into two parts – one of them for the real part, and the other one for the imaginary part:

$$\psi_{Morlet\ real}(t,\sigma,\eta)=\frac{1}{\sqrt{\pi}}\cdot e^{-\beta^2\cdot\frac{t^2}{2}}\cdot\cos(\omega\cdot t) \quad (7)$$

$$\psi_{Morlet\ imag}(t,\sigma,\eta)=\frac{1}{\sqrt{\pi}}\cdot e^{-\beta^2\cdot\frac{t^2}{2}}\cdot\sin(\omega\cdot t) \quad (8)$$

where β is the shape parameter, balancing the time resolution and the frequency resolution.

Only the real part is usually used. The real part of the Morlet wavelet is a cosine signal decaying exponentially on the left and right side, and its function shape is similar to an impulse. Because of this similarity the Morlet wavelet is widely used in mechanical fault diagnostic applications.
By time translation and scale dilation, a daughter Morlet wavelet is acquired from the mother wavelet:

$$\psi_{Morlet}(t,\sigma,\eta)=\frac{1}{\sqrt{\pi}}\cdot e^{-\beta^2\cdot\frac{t(t-u)^2}{2\cdot s^2}}\cdot\cos\left(\frac{\pi\cdot(t-u)}{s}\right) \quad (9)$$

where s is the scale parameter for dilation and u for time translation. It is possible to construct, by selecting parameters s and u, a daughter Morlet wavelet closely matching the shape of a mechanical impulse.
It is required to first define the location and shape of the frequency band corresponding to the impulses in order to define the impulses by means of filtering. Location and shape of the daughter Morlet wavelet are controlled by scale s and parameter β. Due to this, it is possible to, by optimising the two parameters for a daughter wavelet, build an adaptive wavelet filter. The selection of the mother wavelet that adapts best to the signal to be isolated was dealt with by several researchers [20, 22, 23]. It is not required to carry out optimal wavelet reconstruction but to find the best daughter wavelet. Differences between single- and double-sided Morlet wavelets were dealt with by Wang [21]. Their frequency spectra are quite different. A real impulse is usually non-symmetric, and, consequently, the right-hand side of Morlet wavelet was selected to be used as the basis. Such wavelets should be most appropriate to match the behaviour of hidden impulses.
The fourth standardized moment or Kurtosis was used, which can be applied to detect faults due to its sensitivity to sharp variant structures, e.g. impulses.

The fourth standardized moment is determined as follows:

$$\gamma_2=\frac{\mu_4}{\sigma^4} \quad (10)$$

where μ4 is the fourth moment about the mean and σ is the standard deviation. More often, Kurtosis is determined as the fourth cumulant divided by the square of the second cumulant, which is equal to the fourth moment around the mean divided by the square of the variance of the probability distribution minus 3:

$$\gamma_2=\frac{\kappa_4}{\kappa_2^2}=\frac{\mu_4}{\sigma^4}-3 \quad (11)$$

This is known as excess kurtosis. The "minus 3" above is often considered a correction, making kurtosis of the

normal distribution equal to zero. Furthermore, on the grounds of the use of the cumulant, if Y is the sum of n independent random variables, all with the same distribution as X:

$$\gamma_2[Y] = \frac{\gamma_2[X]}{n} \quad (12)$$

The complexity of the equation would increase if kurtosis was defined as μ4 / σ4. In relation to a sample of n values, the sample kurtosis is as follows:

$$\gamma_2 == \frac{\frac{1}{n}\sum_{i=1}^{n}(x_i - \bar{x})^4}{\left(\frac{1}{n}\sum_{i=1}^{n}(x_i - \bar{x})^2\right)^2} - 3 \quad (13)$$

xi is the i-th value, and $\bar{x}$ is the sample mean.
The kurtosis increases with the impulse in signals. Consequently, it is possible to use kurtosis as a performance criterion of a Morlet wavelet.
The procedure of achieving the appropriate wavelet is as follows:
1. In order to produce different daughter wavelets, modify the parameters s and β.
2. Calculate the kurtosis for each daughter wavelet.
3. To identify hidden impulses, it is very appropriate to use parameters s and β corresponding the largest kurtosis.

3. WAVELET DE-NOISING

The aim of wavelet threshold de-noising method, which was introduced by Donoho [12], is to remove independent and identically distributed Gaussian noise. A signal series $x(t)=\{x_1(t), x_2(t) \ldots x_n(t)\}$, which is acquired using a sensor, consists of impulses and noise. It is possible to express $x(t)$ as follows:

$$x(t) = p(t) + n(t) \quad (14)$$

where $p(t)=\{p_1(t), p_2(t) \ldots p_n(t)\}$ denotes the impulses to be determined, whereas $n(t)=\{n_1(t), n_2(t) \ldots n_n(t)\}$ denotes the noise with mean zero and standard deviation σ.
It is assumed by all traditional methods that noise properties are known, meaning that the noise is independent and identically distributed. In industrial applications, however, some data on the signal to be detected is often available but the exact behaviour of the noise is not known. The maximum likelihood estimation de-noising method is suitable for non-Gaussian data.
Prior information on the impulse probability density function is taken into consideration in a specific threshold rule, based on the maximum likelihood estimation method. As to this rule, it is not necessary that the noise is independent and identically distributed Gaussian. It is, however, required to know in advance the probability density function of the impulse to be defined.
Hyvarinen introduced the so-called ''sparse code shrinkage'' method, which estimates non-Gaussian data under noisy conditions and is based on the maximum likelihood estimation principle [16].
For a very sparse probability density function, Hyvarinen [16] used the following function to represent a sparse distribution:

$$p(s) = \frac{(\alpha+2)\cdot(0.5\cdot\alpha\cdot(\alpha+1))^{0.5\cdot\alpha+1}}{2\cdot d\cdot\left(\sqrt{0.5\cdot\alpha(\alpha+1)} + \left|\frac{s}{d}\right|\right)^{\alpha+3}} \quad (15)$$

where d indicates the standard deviation of the impulse to be isolated, whereas α indicates the parameter controlling the sparseness of the probability density function.
For an impulse, in relation to which the probability density function can be represented by Eq. (10), Hyvarinen used the sparse shrinkage threshold rule [16]:

$$g(u) = sign(u)\max\left(0\ ,\ 0.5\cdot\left(|u| - a\cdot d\right) + 0.5\cdot\sqrt{\left(|u| - a\cdot d\right)^2 - 4\cdot\sigma^2\cdot(\alpha+3)}\right) \quad (16)$$

where $\sigma = \sqrt{0.5\cdot\alpha\cdot(\alpha+1)}$ indicates the standard deviation of the noise.
Due to the similarity between a Morlet wavelet and an impulse, a wavelet transform is adopted. This is done using the following steps:
1. To perform a wavelet transform for the signal series $x(t)$, use the Morlet wavelet with appropriate shape. To obtain the wavelet coefficients, use the Eq. (1).
2. To shrink the wavelet coefficients, use the threshold rule from Eq. (16).
3. Perform the inverse transform of the shrunken wavelet coefficients. The result represents an approximation to the impulse to be isolated. Let $W\ x(u,s)$ be reconstructed coefficients. Then, to purify the signal, use the following equation [10]:

$$x(t) = \frac{1}{C_\psi}\cdot\int_{-\infty}^{+\infty}\int_{-\infty}^{+\infty} W\ x(u,s)\cdot\frac{1}{\sqrt{s}}\cdot\psi\left(\frac{t-u}{s}\right)\cdot du\cdot\frac{ds}{s^2} \quad (17)$$

4. PRACTICAL EXAMPLE

All the measurements were carried out in the test plant, shown in Fig. 1, of the Computer Aided Design Laboratory of the Faculty of Mechanical Engineering, University of Maribor.
A single stage gear unit EZ6.B3.132 produced by Strojna Maribor was used. A helical gear unit with straight teeth was integrated into the gear unit [11]. Tests were performed under constant loads. The pinion had 19 and the wheel 34 teeth. Each gear unit had a carburised spur gear pair of module 4 mm. The presented results are in relation to a nominal pinion torque of 30 Nm and nominal pinion speed of 1200 rpm (20 Hz). This is a very typical

load condition for this type of gear units in industrial applications. Accelometers were fixed on the housings to measure vibrations.

Fig. 1. Laboratory test plant

A ground gear pair, which is shown in Fig. 2, was a standard gear pair, with teeth quality 6, but it had a crack in a tooth root of a pinion. The crack was 4.5 mm long. Measurements were carried out in the operating conditions normally associated with this type of a gear unit. The whole measurement process and preparations for analysis are described in [11].

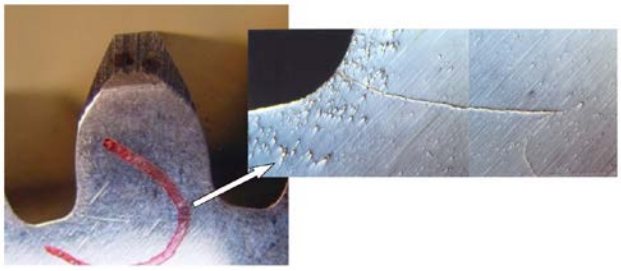

Fig. 2. Pinion with a fatigue crack in the tooth root [1]

Normalised and square values of amplitudes of wavelet coefficients are represented by the Morlet wavelet function. The connection between the scale and frequency is established, thus, the representation is performed in a time-frequency domain. This is very appropriate when it comes to technical diagnostics, as it is much simpler to establish adequate characteristics in time-frequency domain (frequency scalogram) than in time-scale domain (scalogram). Based on normalization, the transform matches the Parseval characteristic of energy preservation, which means that the energy of wavelet transform equals the energy of the original signal in time domain.

For analysis, the continuous wavelet transform was used with the following parameters: $\eta = 6$ and $\sigma = 1$. The representation of the frequency scalogram is given in the form of wavelet coefficients or their square values. Only a part of the signal, which represents one whole rotation of the gear (of a pinion with a crack), taking 50 ms, was used for analysis.

On the basis of the figures, in the frequency scalogram, it is evident that no particularities indicating local changes can be noted in case of the faultless gear; this applies for a normal representation (Fig. 3) of wavelet coefficients and for a square representation (Fig. 4) of wavelet coefficients. In relation to normal representation of wavelet coefficients (Fig. 3), the resolution is much better in the lower frequency area, where the reaction of each single tooth at the frequency of 380 Hz is expressed.

In relation to the signal produced by a gear with a crack, it is possible to notice a local change in wavelet coefficients, at 11 ms, in frequency scalograms with square representation (Fig. 5). It is very difficult to identify the changes (Fig. 6) in normal representation of wavelet coefficients. In relation to normal representation of wavelet coefficients (Fig. 5), an expressed increase in the amplitude can be observed at 11 ms, in the area of the 7th harmonics of the meshing frequency. In concern to the square representation of wavelet coefficients (Fig. 6), a local increase in the amplitude is expressed.

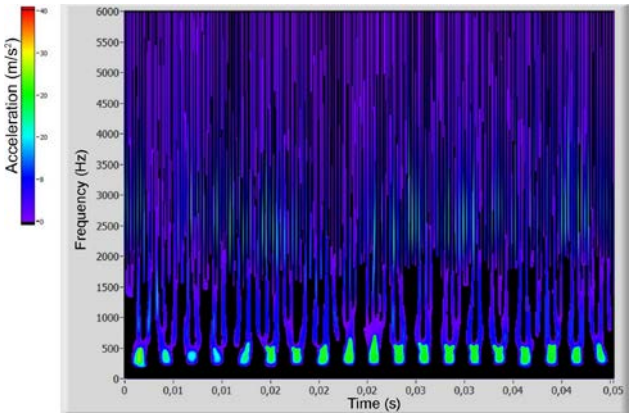

Fig. 3. Frequency scalogram of wavelet coefficient of the reference gear unit

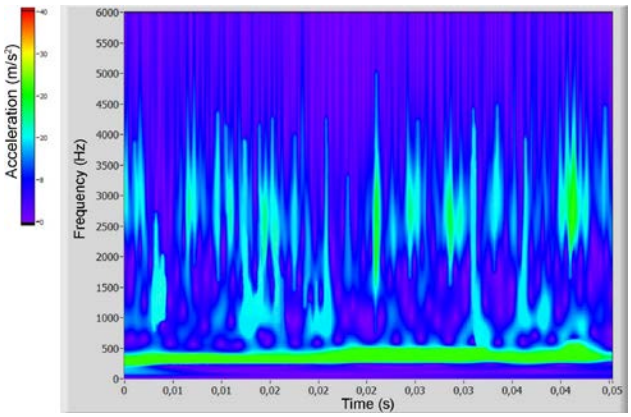

Fig. 4. Frequency scalogram of square wavelet coefficient of the reference gear unit

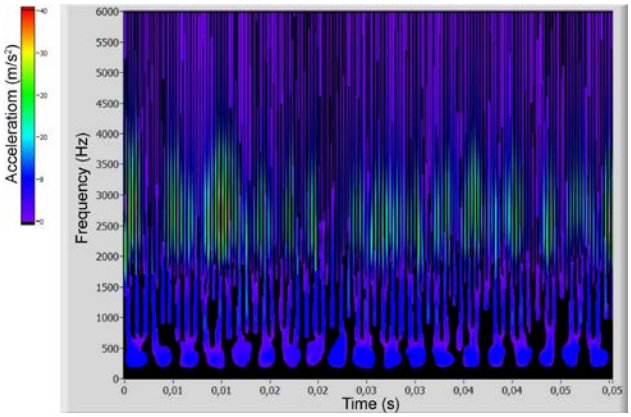

Fig. 5. Frequency scalogram of wavelet coefficient of the gear unit with a gear with a crack in a tooth root

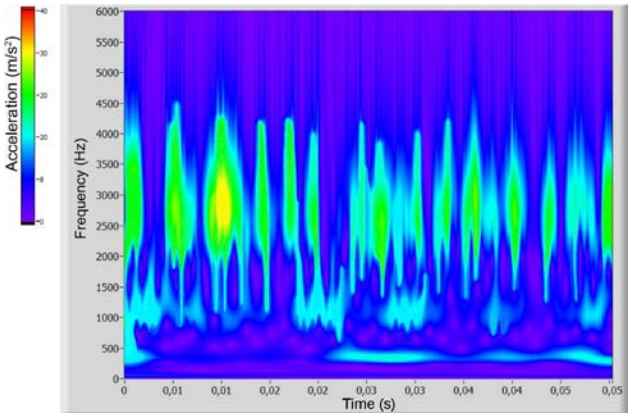

Fig. 6. Frequency scalogram of square wavelet coefficient of the gear unit with a gear with a crack in a tooth root

Morlet wavelet was used to obtain the adaptive wavelet filter. The graph of the scale, β and kurtosis relationship is presented in Fig. 7. The kurtosis is very sensitive to the value β. Let parameter β vary from 0.1 to 5 with a step size of 0.1, and the scale from 1 to 40 with a step size of 0.11. The largest kurtosis value of 5.2 is acquired when β=0.4 and the scale equals 25, as shown in Fig.7. As a de-noising method, the Morlet wavelet is used. Eq. (15) with $\alpha=0.1$ can be used to approximate the impulse probability density function. For each scale, MAD/0.6745 is used as the noise deviation estimator. For Morlet wavelet, the same parameters are applied as described before. Measured signals of vibrations of a faultless gear and of vibrations of a gear with a crack in the tooth root are presented in Figures 8 and 9. Fig. 10 shows de-noising signals of a faultless gear. It can be noted that no impulses exist in the signals, whereas Fig. 11 shows results of filtering with optimized wavelet filter for signals of a gear with a crack; in these signals it is possible to observe impulses at 11 ms also after the noise has been removed.
The signal length is 50 ms, representing one rotation of the pinion. 19 teeth are along the circumference. The increased amplitude is located at 11 ms and belongs to the fourth tooth in the direction of rotation from the reference positional point of the gear unit.

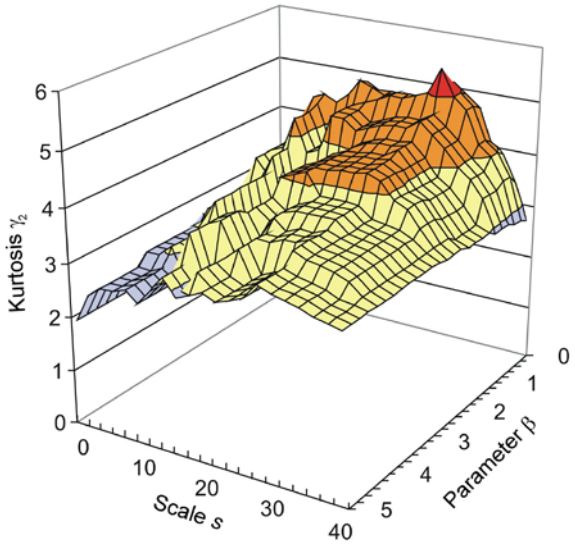

Fig. 7. Graph of the scale, β and kurtosis distribution

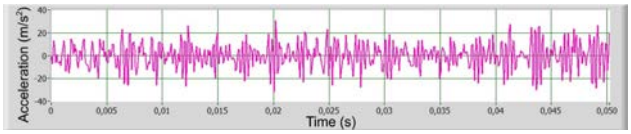

Fig. 8. Measured signal of vibrations of a faultless gear unit

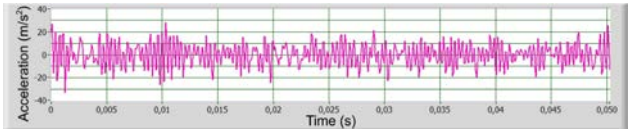

Fig. 9. Measured signal of vibrations of a gear with a pinion with a crack

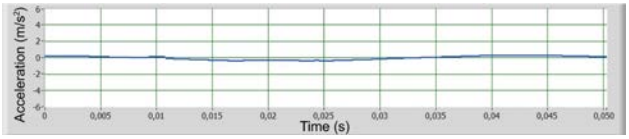

Fig. 10. With Morlet wavelet de-noised signal of vibrations of a faultless gear unit

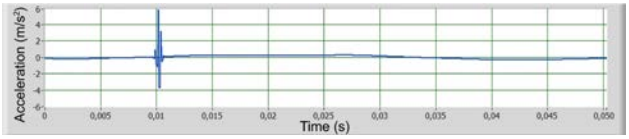

Fig. 11. With Morlet wavelet de-noised signal of vibrations of a gear with a pinion with a crack

5. CONCLUSION

In a very short time, on the basis of adaptive wavelet transform, changes can be identified and the presence of a damage, at the level of an individual tooth, can be determined. When determining local changes in gears, adaptive wavelet de-noising methods are very helpful. Optimised wavelets with Kurtosis match impulses very well. As a result, impulses hidden in noise signals can be identified, using the wavelet transform. In relation to this method, the maximum likelihood estimation threshold rule and prior information on the probability density function of the signals to be determined are applied. This method is used to extract impulses from practical engineering signals and it yields very good results.

In relation to life cycle design, it is possible to monitor the actual condition of a device and its vital component parts, which can have a considerable impact upon the operational capability, based on an adequate method or criterion. Undoubtedly, in-time detection of faults and damages considerably improves the reliability of operation control. If detection of faults is reliable to a great extent, the prediction of the remaining life cycle of a gear unit can be improved.

REFERENCES

[1] Belsak A, Flasker J. **Detecting cracks in the tooth root of gears.** Engineering Failure Analysis 2007; 14(8). p. 1466-1475

[2] Adewusi S, AI-Bedoor B. **Wavelet analysis of vibration signals of an overhang rotor with a propagating transverse crack.** Journal of Sound and Vibration 2001; 246(5). p. 777–793.

[3] Bruce AG, Donoho DL et al. **Smoothing and Robust Wavelet Analysis**, Proceedings in Computational Statistics, 11th Symposium, Vienna: 1994. p. 531–547.

[4] James I Taylor. **The Vibration Analysis Handbook**. Vibration Consultans; 1994.

[5] Smith J Derrek. **Gear Noise and Vibration**. New York: Marcel Dekker; 1999.

[6] Victor C Chen, Hao Ling. **Time-Frequency Transforms**. Boston: Artech Hause Publishers; 2002.

[7] Fladrin P. **Time-Frequency/Time-Scale Analysis**. San Diego: Academic Press; 1999.

[8] Mertins A. **Signal Analysis**. New York: John Wiley & Sons Inc; 1999.

[9] Qian S, Chen D. **Joint Time-Frequency Analysis**. Upper Saddle River: Prentice Hall; 1996

[10] Mallat S. **A Wavelet Tour of Signal Processing**. San Diego: Academic Press; 1999.

[11] Belsak A. **Time-Frequency Analysis of the Condition of Gear Units** (Abstract in English). Doctoral Thesis, University of Maribor, Faculty of Mechanical Engineringg: 2006.

[12] Donoho D L. **De-noising by Soft-Thresholding**. IEEE Trans. Inf. Theory 1995; 41(3). p. 613– 627.

[13] Donoho D L, Johnstone I M. **Ideal Spatial Adaptation by Wavelet Shrinkage**. Biometrika 1994, 81(3). p. 425–455.

[14] Fan J Q, Hall P, Martin M A, Patil P. **On Local Smoothing of Nonparametric Curve Estimators**. J. Am. Stat. Assoc 1996, 91. p. 258 –266.

[15] Donoho D L, Johnstone I M. **Adapting to Unknown Smoothness via Wavelet Shrinkage.** J. Am. Stat. Assoc. 1995, 90. p. 1200–1224.

[16] Hyvarinen A. Sparse Code Shrinkage: **Denoising of Nongaussian Data by Maximum Likelihood Estimation**. Neural Comput. 1999, 11(7). p. 1739– 1768.